Research Square

Preprints are preliminary reports that have not undergone peer review.
They should not be considered conclusive, used to inform clinical practice,
or referenced by the media as validated information.

Genomic Characterization and In Vivo Therapeutic Potential of a Siphoviridae Bacteriophage against Multidrug-Resistant Streptococcus pyogenes: Effects on Immunity, Oxidative Status, and Histopathology in Nile Tilapia (Oreochromis niloticus)

Alshimaa A. Khalil
Zagazig University
Enas A. Ramadan
National Institute of Oceanography and Fisheries (NIOF)
Kasim Sakran Abass
University of Kirkuk
Rania Ali
Zagazig University
Rewan Abdelaziz
rewan_abdelaziz92@yahoo.com

Ain Shams University

Research Article

Keywords: Streptococcus pyogenes PX884326, Siphoviridae, Whole Genome Sequencing (WGS), Nile tilapia

Posted Date: November 23rd, 2026

DOI: https://doi.org/10.21203/rs.3.rs-10943399/v1

License: This work is licensed under a Creative Commons Attribution 4.0 International License.
Read Full License

Additional Declarations: No competing interests reported.

Genomic Characterization and In Vivo Therapeutic Potential of a Siphoviridae Bacteriophage against Multidrug-Resistant *Streptococcus pyogenes*: Effects on Immunity, Oxidative Status, and Histopathology in Nile Tilapia (*Oreochromis niloticus*)

Alshimaa A.Khalil[1], Enas A. Ramadan[2], Kasim Sakran Abass[3], Rania Ali[4], Rewan Abdelaziz[5]*

[1] Department of Aquatic Animal Medicine, Faculty of Veterinary Medicine, Zagazig University, Zagazig 44511, Egypt

[2] National Institute of Oceanography and Fisheries (NIOF), El Qanater El Khayreya, Al Qalyubiyah, Egypt.

[3] Department of Physiology, Biochemistry, and Pharmacology; College of Veterinary Medicine; University of Kirkuk; Kirkuk 36001, Iraq.

[4]Department of Microbiology, Faculty of Science, Zagazig University, Zagazig, 44511, Egypt.

[5]Department of Microbiology, Faculty of Science, Ain Shams University, Cairo, 11517, Egypt

* Corresponding authors.

E-mail address: rewan_abdelaziz92@yahoo.com (Rewan Abdelaziz)

Abstract

The worldwide emergence of multidrug-resistant (MDR) *Streptococcus pyogenes* (*S. pyogenes*) has created an urgent need for alternative antimicrobial approaches. In the present study, a temperate bacteriophage (SPB) was induced from a clinical MDR *S. pyogenes* isolate and molecularly identified through phylogenetic analysis (Accession No. PX884326). Transmission Electron Microscopy (TEM) classified the phage within the Siphoviridae family. Physicochemical characterization demonstrated high stability under different environmental conditions, including temperatures up to 55°C, UV exposure up to 90 cm, and optimal activity at pH 7. Whole Genome Sequencing (WGS) further revealed its genetic architecture, confirming its lytic potential and the absence of virulence-associated genes. The antibacterial efficacy and therapeutic potential of SPB were evaluated both in vitro and in vivo using Nile tilapia (*Oreochromis niloticus*) as an experimental model. Fish were allocated into four groups: a negative control, a phage-treated group, an infected control group, and an infected phage-treated group. Phage treatment significantly improved survival rates and alleviated the detrimental effects of *S. pyogenes* infection on hepatorenal biomarkers, nonspecific immune responses, and antioxidant activities. Nitric oxide (NO) levels and lysozyme (LYZ) activity were markedly enhanced, while antioxidant defenses were significantly improved in phage-treated fish. Histopathological examination demonstrated substantial recovery of liver, intestine, and spleen tissues, with marked reductions in bacterial-induced lesions and inflammatory responses compared with untreated infected fish. Overall, SPB exhibited potent antibacterial activity, high stability, and a favorable safety profile, highlighting its promise as an effective biological alternative to conventional

antibiotics for the control of pyogenic infections in aquaculture and other clinical settings.

Keywords: *Streptococcus pyogenes* PX884326**;** *Siphoviridae***;** Whole Genome Sequencing (WGS); Nile tilapia**.**

1. Introduction

The rapid emergence and spread of antimicrobial resistance (AMR) has become a major global health challenge, threatening the effectiveness of conventional antibiotics and undermining decades of progress in infectious disease management. Among the pathogens of increasing concern is *Streptococcus pyogenes* (Group A Streptococcus), a highly invasive Gram-positive bacterium responsible for a wide spectrum of diseases ranging from mild infections such as pharyngitis to severe invasive conditions including necrotizing fasciitis and streptococcal toxic shock syndrome (Walker et al., 2022). Although β-lactam antibiotics remain effective against many strains, the emergence of multidrug-resistant (MDR) isolates, particularly those exhibiting resistance to macrolides and tetracyclines, has created a significant therapeutic challenge (Efstratiou and Lamagni, 2021).

The increasing prevalence of antibiotic-resistant bacteria has stimulated the search for alternative antimicrobial approaches. Among the most promising strategies is bacteriophage therapy, which utilizes viruses that specifically infect and lyse bacterial cells. Unlike conventional antibiotics, bacteriophages exhibit high host specificity, enabling targeted elimination of pathogenic bacteria while preserving beneficial microbiota and minimizing environmental impact (Gordillo Altamirano and Barr, 2021; Joerger, 2020). Consequently, phage therapy has gained considerable attention as a sustainable and effective biological tool for combating MDR bacterial

infections in both medical and veterinary applications (Kumar et al., 2018; Sillankorva et al., 2008; Kropinski, 2024).

The therapeutic success of bacteriophages depends largely on their biological characteristics, genomic composition, and environmental stability. Members of the *Siphoviridae* family, characterized by their long non-contractile tails, have been widely recognized for their genetic stability and antibacterial potential (Ackermann, 2011). Furthermore, the ability of phages to withstand environmental stresses such as temperature fluctuations, ultraviolet radiation, and pH variations is essential for their practical application in disease control programs (Joerger, 2020). Advances in whole-genome sequencing have also facilitated the identification of phage genetic traits, enabling the assessment of their safety and therapeutic suitability through the detection of virulence- and resistance-associated gene (Suvarna et al., 2018; Tan et al., 2022; Weisburg et al., 1991; Clinical and Laboratory Standards Institute, 2023).

- In parallel, aquaculture has become one of the fastest-growing food production sectors worldwide, with Nile tilapia (*Oreochromis niloticus*) representing one of the most economically important cultured fish species due to its rapid growth, high adaptability, and market value (Kwikiriza et al., 2025). However, intensive farming practices have increased fish susceptibility to bacterial diseases, leading to substantial economic losses and compromised fish health (Gundi et al., 2025). Streptococcal infections are among the most significant bacterial diseases affecting cultured fish, causing severe physiological disturbances, impaired hepatorenal function, suppression of nonspecific immune responses, oxidative stress, and extensive tissue damage in vital organs such as the liver, kidney, and spleen (Abdallah et al., 2024). Infection with *S. pyogenes* has been associated with mortality rates of up to 60% in

infected fish populations in Egypt (Abou El-Gheit, 2005 ; Sahoo and Rukmini, 2014; Coulombe and Favreau, 1963; Larsen, 1972; Aebi, 1984; Nishikimi et al., 1972). Transmission mainly occurs through skin injuries and abrasions. The pathogen can spread through contaminated water, infected fish, and the use of infected fish as feed, facilitating disease outbreaks among cultured and wild fish populations (Kim et al., 2007).

Fish models have emerged as valuable in vivo systems for evaluating novel antimicrobial agents because they possess well-developed innate and adaptive immune systems while offering practical and ethical advantages over traditional mammalian models (Sullivan and Lehman, 2021). Moreover, the use of fish models is particularly relevant for investigating alternative disease-control strategies in aquaculture, where excessive antibiotic use has contributed to the development of resistant bacterial populations and environmental contamination.

Therefore, the present study aimed to induce and characterize a bacteriophage (SPB) isolated from a multidrug-resistant *Streptococcus pyogenes* strain through morphological, physicochemical, and genomic analyses. In addition, the study evaluated the in vivo therapeutic efficacy of the phage in Nile tilapia by assessing its effects on fish survival, hepatorenal biomarkers, nonspecific immune responses, antioxidant status, and histopathological alterations. The findings contribute to the growing body of evidence supporting bacteriophages as safe, stable, and effective biological alternatives to conventional antibiotics for the control of MDR bacterial infections.

2. Materials and Methods

1. Isolation and Primary Identification

A pathogenic strain of *Streptococcus pyogenes* was recovered from naturally infected Nile tilapia (*Oreochromis niloticus*) at the Department of Aquatic Animal Medicine, Faculty of Veterinary Medicine, Zagazig University, Egypt. The isolate was identified using standard biochemical assays and confirmed using the VITEK® 2 system (bioMérieux, Marcy l'Etoile, France). **Bergey's Manual of Systematic** Bacteriology (Garrity et al., 2005).

2. Antibiotic Susceptibility Testing (In Materials and Methods)

The antibiotic susceptibility profiles of the 44 *S. pyogenes* clinical isolates were determined using the Kirby-Bauer disc diffusion method on Mueller-Hinton agar supplemented with 5% sheep blood. A panel of antibiotics was selected based on clinical relevance, including: Rifampin (RA), Ceftriaxone (CRO), Ceftazidime (CAZ), Oxacillin (OX), Ciprofloxacin (CIP), Sulfamethoxazole-Trimethoprim (SXT), Fusidic Acid (FA), Teicoplanin (TEC), Tigecycline (TGC), Clindamycin (DA), Linezolid (LNZ), Fosfomycin (FF), Tetracycline (TE), and Erythromycin (E). The zones of inhibition were measured after 24 hours of incubation at 37°C. The results were interpreted as Susceptible (S), Intermediate (I), or Resistant (R) according to the clinical breakpoints established by the **Clinical and Laboratory Standards Institute (CLSI, 2023)** guidelines. Isolates resistant to three or more different classes of antimicrobials were classified as Multi-Drug Resistant (MDR).

3. Molecular Identification and Phylogenetic Analysis

Genomic DNA was extracted using a commercial kit. Molecular confirmation was achieved by amplifying the 16S rRNA gene using the universal primers 27F and 1492R, according to the protocol described by **Weisburg** *et al***. (1991)**. Phylogenetic analysis was performed using MEGA X software **(Kumar** *et al***., 2018)** to determine

the evolutionary position of the strain, which was deposited in GenBank under Accession No. PX884326.

4. Prophage Induction and Purification

Lysogenic phages were induced from the MDR *S. pyogenes* isolate following the chemical induction method using Mitomycin C, as optimized by **Clokie and Kropinski (2009)**. The induced lysate was centrifuged and filtered through a 0.22 μm syringe filter. Phage titers were determined using the double-layer agar (DLA) technique as described by **Kropinski et al. (2009)**.

5. Morphological Characterization (TEM)

The purified phage particles were concentrated and applied to carbon-coated copper grids. Negative staining was performed using **2% uranyl acetate (v/v)** according to the methodology of **Ackermann (2009)**. Visualization was carried out using a **Transmission Electron Microscope (TEM)** to classify the phage based on the International Committee on Taxonomy of Viruses (ICTV) standards.

6. Physicochemical Stability Assays

The resilience of the induced phage was evaluated against various environmental stressors following the parameters set by **Joerger (2020)**:

- **Thermal Stability:** Phage stability was tested at temperatures up to **55°C**.
- **pH Stability:** Survival was measured across a pH range of 2–12, with optimal stability recorded at **pH 7**.
- **UV Exposure:** Phage resistance to ultraviolet radiation was assessed for durations up to **90 minutes**, following the UV-stability protocol of **Sillankorva** ***et al*****. (2008)**.

7. Host Range (Host Strain)

Bacteriophage**:** Phage lysate with an initial titer of 9.5 ×10^^{9} PFU/ml. Host Cells: Log-phase bacterial culture (10^^{8}CFU/ml). Incubation**:** Water bath set at 37°C (or your specific incubation temperature). Stop Solution/Method: Ice-cold TSB or Chloroform (if used) to stop the adsorption process at specific time intervals (0, 1, 2, 3, 4, 5 min). Centrifugation**:** High-speed centrifuge to separate adsorbed phages from free phages in the supernatant (**Hyman & Abedon 2010)**.

8. Adsorption Rate

Bacteriophage: Phage lysate with an initial titer of 9.5 ×10^^{9} PFU/ml. Host Cells: Log-phase bacterial culture (10^^{8} CFU/ml). Incubation: Water bath set at 37°C (or your specific incubation temperature). Stop Solution/Method: Ice-cold TSB or Chloroform (if used) to stop the adsorption process at specific time intervals (0, 1, 2, 3, 4, 5 min). Centrifugation: High-speed centrifuge to separate adsorbed phages from free phages in the supernatant **(Kropinski, 2024).**

9. One-Step Growth Curve Phage and Host: Purified Phage and its specific E host strain

Infection Ratio (MOI): Multiplicity of Infection (usually 0.01 or 0.1) to ensure single-step infection. Adsorption period: Pre-incubation for 10–15 minutes to allow phage attachment. Dilution Series: Several tubes of pre-warmed TSB for serial dilutions to prevent further adsorption. Double-Layer Agar (DLA) Method: Bottom Layer: 1.5% Agar (Hard agar). Top Layer: 0.7% Soft agar (used to mix the phage-bacteria sample). Petri Dishes: For plaque assay at each time interval (from 0 to 70 min) **(Kropinski, 2024).**

10. Whole Genome Sequencing (WGS) and Bioinformatics

Phage DNA was extracted using the phenol-chloroform method. **Whole** Genome Sequencing (WGS) was performed on an Illumina platform. *De novo*

assembly and functional annotation were conducted using the RAST pipeline **(Aziz *et al*., 2008)** and PHASTER **(Arndt et al., 2016)** to identify lytic genes and ensure the absence of antibiotic resistance genes (ARGs).

11. Fish and rearing conditions

Nile tilapia (N = 120; mean body weight 50.5 ± 0.5 g) were clinically examined and handled in accordance with the guidelines of the Canadian Council on Animal Care (CCAC, 2005). Fish were randomly stocked in 100-L glass aquaria containing dechlorinated tap water and acclimated for two weeks prior to experimentation. During acclimation, fish were fed a basal diet and continuous aeration was provided using air compressors and air stones. Water was renewed daily. Throughout the experimental period, water quality parameters were maintained according to APHA (1998) under a controlled photoperiod of 12 h light/12 h dark: temperature 28.3 ± 1.1°C, dissolved oxygen 7.6 ± 0.3 mg/L, pH 6.9 ± 0.1, and total ammonia 0.035 ± 0.01 mg/L.

12. Challenge test

The median lethal dose (96-h LD_{50}) of *S. pyogenes* was determined using 110 fish distributed into five challenged groups and one control group (20 fish per group; 10 fish per replicate). Fish were fasted for 24 h before infection. Challenged fish received intraperitoneal (I/P) injections of 0.2 mL of serial bacterial dilutions (10^5–10^9 CFU/mL), whereas the control fish were injected with sterile phosphate-buffered saline (PBS). Fish were observed for 96 h without feeding, and 25% of the water was exchanged daily. Mortality was recorded at 24, 48, 72, and 96 h post-challenge. The LD_{50} was estimated by Probit analysis using SPSS (v18). The calculated LD_{50} was 4.7×10^9 CFU/mL. Therefore, a sublethal dose of 1.5×10^8 CFU/mL was selected for the treatment experiment.

13. Experimental design

Fish were randomly allocated into four groups with three replicates each (10 fish per replicate):

- **G1:** negative control (no bacteria, no phage)
- **G2:** positive control (*S. pyogenes* only)
- **G3:** phage only
- **G4:** infected + phage treated

Fish in the infected groups were I/P injected with 0.2 mL of *S. pyogenes* suspension (1.5×10^8 CFU per fish). To ensure establishment of infection, phage therapy was initiated 24 h post-infection. This interval allowed bacterial colonization and onset of disease, thereby representing a therapeutic rather than prophylactic regimen.

Fish in G3 and G4 were immersed in dechlorinated, aerated water containing bacteriophage (2×10^8 PFU/mL) for 1 h daily for five consecutive days. To obtain a theoretical estimate of the multiplicity of infection (MOI) expected under immersion conditions, the injected bacterial load (1.5×10^8 CFU/mL; 0.2 mL per fish $\approx 3 \times 10^7$ CFU per fish) was considered relative to the phage concentration applied in water (2×10^8 PFU/mL). Evidence from immersion-based delivery systems indicates that only a limited fraction of phage particles can penetrate host tissues, commonly estimated at approximately 0.1–1%, depending on epithelial permeability and infection status. Accordingly, the effective in vivo MOI in the present trial was projected to fall within a range of approximately 0.007–0.07. This level was regarded as sufficient to initiate phage replication at the infection site. After each exposure, fish were returned to their tanks and monitored for clinical signs, survival, and health indicators.

Stocking density was maintained at 10 fish per 120-L aquarium. Water temperature (28 ± 1°C), pH (7.0 ± 0.2), and dissolved oxygen (~7 mg/L) were maintained. After each exposure, fish were returned to their tanks and monitored for clinical signs, survival, and health indicators. The phage protocol followed Janelidze et al. (2022) with minor modifications.

14. Sampling

Five fish per aquarium were randomly netted and anesthetized with eugenol (50 μL/L) (da Paz et al., 2004) for less than 3 min. Blood was collected from the caudal vessels using sterile syringes without anticoagulant and centrifuged at 3000 rpm for 10 min to obtain serum, which was stored at -20°C until analysis. Liver, intestine, and spleen samples were aseptically excised for histopathological investigations.

15. Hepatorenal function markers

Serum AST and ALT activities were determined according to Sahoo et al. (Sahoo and Rukmini, 2014). Urea and creatinine levels were assessed following Copfuulombe and Favreau (1963) and Larsen (1972), respectively.

16. Antioxidant and innate immune parameters

Total antioxidant capacity (TAC) and catalase (CAT) were measured as previously described (Aebi, 1984)]. Superoxide dismutase (SOD) activity was estimated following Nishikimi et al. (1972), and reduced glutathione (GSH) according to Beutler et al. (1963). Lysozyme activity was determined turbidimetrically (Ellis, 1990), whereas nitric oxide (NO) levels were quantified using the method of Montgomery and Dymock, (1961) ; Beutler et al., 1963; Ellis, 1990; Bancroft et al., 2013; Stevens, 2013).

.

17. Histopathological examination

Tissues were fixed in 10% neutral buffered formalin for 48 h, dehydrated through ascending ethanol concentrations, cleared in xylene, and embedded in paraffin. Sections (5 μm) were prepared using a microtome (Leica RM2155) and stained with hematoxylin and eosin for microscopic examination (Bancroft et al., 2013). Photomicrographs were captured using a digital microscope camera.

18. Statistical analysis

Data were analyzed using SPSS version 18. Differences among groups were evaluated by one-way ANOVA followed by Duncan's multiple range test at a significance level of $P < 0.05$ (Stevens, 2013).

3. Results

1. Clinical Isolation and Antibiotic Susceptibility Profile

To identify the most suitable host for prophage induction, an extensive antibiotic susceptibility screening was conducted using the Kirby-Bauer disk diffusion method. The isolates exhibited varying degrees of resistance, with a significant number showing Multi-Drug Resistance (MDR) profiles. The following table summarizes the resistance patterns of the most significant isolates. Isolate RE13 demonstrated the highest resistance frequency and was subsequently used for bacteriophage induction.

The figure1 illustrates the appearance of clear plaques surrounding specific antibiotic discs, signifying the transition of lysogenic phages to the lytic cycle as a response to chemical stress

2. Morphological and Biochemical Characterization (Phenotypic Identification)

All 44 clinical isolates were subjected to a series of standard microbiological tests to confirm their identity. The results consistently identified the isolates as *Streptococcus pyogenes*.

3. Molecular Identification and Phylogenetic Analysis

Genetic Confirmation: "After achieving these results and observing the formation of clear plaques, I proceeded to identify and characterize this specific bacterial **RE13**."16S rRNA gene sequencing confirmed the isolate as ***Streptococcus pyogenes***. **Phylogenetic Relationship:** The constructed tree shows that the isolate **(8) PX884326.1 (RE13)** clusters closely with the global reference strain **JP1 (PV583599.1)**, exhibiting nearly **100% sequence identity as shown in Fig.2**. **Evolutionary Lineage:** The strain shares a direct common ancestor with documented GenBank strains **S4, S7, and 3.4**, validating its taxonomic position within the *S. pyogenes* species **as shown in Fig.3**.

The micrograph reveals the morphological characteristics of the isolate, showing an icosahedral head (approximately 62 nm in diameter) and a long, non-contractile, flexible tail (approximately 115 nm in length). Based on these morphological features, the phage belongs to the *Siphoviridae* family.

Physicochemical Stability Assays of Phage

The thermal stability of phage was evaluated at temperatures ranging from 30°C to 100°C. The results indicated that the phage maintained full stability up to 40°C. A significant decline in viability was observed starting from 50°C, followed by complete inactivation at temperatures of 70°C and above as shown in figure 4.

The phage showed maximum stability in the alkaline range, specifically at pH 7.0 (9.19 ±0.07Log PFU/ml). Significant reduction in phage titer was observed at extreme acidic (pH 2.0-3.0) and extreme alkaline (pH 11.0-13.0) conditions, where complete inactivation occurred at figure 5.

The data shows that the phage maintained its full stability for the first 40 minutes, followed by a gradual decrease in the titer. Complete loss of infectivity (total inactivation) was reached after 100 minutes of continuous UV exposure as shown in figure 6.

The host range of phage was evaluated against 44 different isolates. The results, summarized in Table 3, revealed that the phage possesses a relatively broad lytic spectrum. Out of the 44 isolates tested, was able to infect 11 isolates (approximately 25% of the tested strains) with varying degrees of lytic activity.

Strong lytic activity (+++), characterized by the formation of clear plaques, was observed against 8 isolates (No. 1, 13, 15, 31, 40, 41, 42, and 44). Moderate infection (++) was recorded for isolates No. 2 and 18, while isolate No. 30 showed weak lytic activity (+). On the other hand, the remaining isolates, including the excluded isolate No. 10, showed complete resistance to phage infection (-). The ability of phage to lyse multiple strains suggests its potential effectiveness as a biocontrol agent against various streptovoccus-related issues or its significance in the microbial ecosystem. The variation in the susceptibility of different isolates might be attributed to differences in the presence of specific surface receptors required for phage adsorption or the existence of intracellular antiviral defense systems in the resistant strains.

The line graph illustrates the rapid reduction of free phage particles over 5 minutes. The initial concentration of 9.5 ×10^9 PFU/ml dropped significantly to 1.0 ×10^6 PFU/ml, demonstrating high adsorption efficiency within the first 2 minutes of incubation.

One-step Growth Analysis: "The growth characteristics of Phage1P were determined through a one-step growth curve. The results showed a latent period of approximately 15 minutes, during which the number of free phages remained stable. This was followed by a sharp rise period between 15 and 35 minutes, indicating the lysis of host cells and the release of new viral progeny. The maximum phage titer was reached at 35 minutes ($8.91\log_{10}$ PFU/ml). Based on these values, the burst size was calculated to be approximately 18.8 phages per infected cell. A secondary increase in titer was observed after 60 minutes, likely representing the initiation of a second infection cycle."

Hepatorenal function indicators

As shown in Table 4, infection with *S. pyogenes* (G3) resulted in a significant elevation ($P < 0.05$) in liver enzymes, including ALT, AST, and ALP, compared to all other groups. The highest values were recorded in G3 (91.33 ± 2.90, 80.33 ± 3.57, and 60.67 ± 10.39 U/L, respectively). In contrast, fish treated with SPB following infection (G4) showed a significant reduction ($P < 0.05$) in these parameters compared to the infected untreated group (G3), although values remained significantly higher than the negative control (G1) and SPB-treated group (G2).

Regarding kidney function markers, creatinine and urea levels were significantly increased ($P < 0.05$) in the infected group (G3) compared to other groups. Treatment with SPB (G4) significantly ameliorated these elevations. The lowest values were observed in G2, indicating a protective or stabilizing effect of SPB.

Antioxidant and immune indicators

Table 5 shows that TAC, SOD, CAT, and GSH levels were significantly decreased ($P < 0.05$) in the infected group (G3) compared to all other groups. Conversely, the SPB-treated group (G4) exhibited a significant improvement in antioxidant status compared to G3. Notably, the highest TAC and SOD values were observed in G2, suggesting that SPB alone may enhance antioxidant capacity.

Significant differences ($P < 0.05$) were observed in lysozyme (LYZ) and nitric oxide (NO) levels among groups. The infected group (G3) showed the lowest values, indicating immunosuppression. In contrast, SPB treatment (G4) significantly increased LYZ and NO levels compared to G3, reflecting partial restoration of immune function. The highest values were recorded in G2.

The effects of *Streptococcus pyogenes* infection and/or its bacteriophage (SPB) treatment on hepatorenal, antioxidant, and immunological parameters in Nile tilapia are presented in Tables 4 and 5.

Clinical signs and postmortem lesions

Gross pathological changes observed in experimentally infected Nile tilapia challenged with *S. pyogenes* are shown in Figure (9). (A) External examination revealed prominent clinical lesions characterized by focal scale detachment, accompanied by extensive cutaneous hemorrhages and severe erosion of the caudal and dorsal fins. These lesions reflect tissue damage, inflammatory responses, and bacterial invasion of the skin and fin structures. (B) The gall bladder appeared markedly enlarged, dark green to blackish in color, and severely congested, suggesting impaired bile flow, vascular congestion, and systemic infection affecting the hepatobiliary system. (C) Internal examination demonstrated generalized congestion of the visceral organs associated with multiple hemorrhagic lesions. The

liver, spleen, and kidney exhibited pronounced vascular engorgement and diffuse hemorrhage, indicating septicemia and widespread circulatory disturbances induced by *S. pyogenes* infection. (D) Severe gill rot was observed, characterized by degeneration and necrosis of the gill filaments, accompanied by a markedly enlarged congested gall bladder. The gill lesions are indicative of impaired respiratory function and extensive tissue destruction resulting from bacterial colonization and inflammatory processes.

Histopathological investigation

Histological examination of the intestinal tissue is shown in Figure 10 that revealed slight degeneration of the intestinal submucosa in G2 (control positive group treated by SPB only in water), accompanied by increased villus height and muscular layer thickness. In contrast, G3 (control positive group infected with *S.pyogenes* without treatment) exhibited severe degeneration of the villous mucosa and submucosa, resulting in villous sloughing, atrophy, and focal areas of necrosis. Group (1) (negative control group) showed intact intestinal architecture with an increased number of goblet cells, mild inflammatory cell infiltration, and enhanced villus height and muscular layer thickness. Meanwhile, Group (4) (infected with *S.pyogenes* and treated by SPB) demonstrated nearly intact intestinal tissue, increased goblet cell numbers, and reduced inflammatory cell infiltration, suggesting a protective effect of phage therapy against tissue damage.

The morphometric analysis in the figure (11A and B) illustrates the mean intestinal villi length and width (μm) in the four experimental groups (G1, G2, G3, and G4). The tallest intestinal villi were observed in **G1**, whereas **G3** exhibited the shortest villi. Variations in villi width among the groups were comparatively smaller than those observed for villi length. Data are presented as mean values (μm)**.**

Histopathological examination of liver and pancreas sections stained with hematoxylin and eosin (H&E) demonstrated distinct pathological alterations among the experimental groups (Fig.12). The **(G1)** exhibited nearly normal hepatic and pancreatic architecture, with only mild congestion of blood vessels and moderate degeneration of hepatocytes and pancreatic acinar cells. The hepatic cords remained generally organized, and the pancreatic tissue preserved its normal structural arrangement despite the presence of slight degenerative changes. The **(G2)** showed moderate histopathological changes characterized by degeneration of hepatocytes and pancreatic tissue, as evidenced by cytoplasmic vacuolation and loss of normal cellular architecture. In addition, marked congestion and dilation of the hepatic vein were observed, indicating vascular disturbances that may be associated with the host immune response or phage administration, while the overall tissue organization remained relatively preserved.

The **(G3)** exhibited the most severe pathological lesions. Liver sections revealed pronounced congestion and marked dilation of the hepatic vein as well as extensive congestion of the hepatic sinusoids, reflecting impaired blood circulation and severe inflammatory responses. Hepatocytes showed prominent fatty degeneration, characterized by the accumulation of intracellular lipid vacuoles that displaced the cytoplasm and nuclei. Numerous hepatocytes displayed pyknotic nuclei, indicating irreversible nuclear condensation and cell death. In addition, the pancreatic

tissue exhibited extensive degenerative changes with disruption of the acinar structure and loss of normal cellular morphology, suggesting significant damage induced by bacterial infection.

In contrast, the infected group treated with bacteriophage **(G4)** demonstrated considerable improvement in tissue morphology compared with the untreated infected group. Although congested blood vessels were still observed, the degree of vascular congestion was less pronounced. Moderate degeneration of hepatic cells and pancreatic tissue persisted; however, the overall hepatic architecture was better preserved, with fewer degenerative and necrotic changes. These findings indicate that bacteriophage treatment effectively reduced the severity of liver and pancreatic damage caused by bacterial infection and contributed to the restoration of normal tissue structure. Overall, the histopathological findings suggest that bacterial infection induced severe hepatic and pancreatic injury characterized by vascular congestion, fatty degeneration, cellular degeneration, and nuclear pyknosis, whereas bacteriophage treatment markedly alleviated these pathological alterations and improved tissue integrity.

The histopathological examination of spleen sections stained with hematoxylin and eosin (H&E) revealed marked differences in splenic architecture among the experimental groups, reflecting the effects of bacterial infection and bacteriophage treatment. The **(G1)** exhibited a normal splenic architecture characterized by well-defined and prominent white pulp surrounded by a normally distributed red pulp. The splenic tissue maintained its normal histological organization without significant pathological alterations, indicating the absence of inflammatory or degenerative changes.

The **(G2)** demonstrated moderate histopathological changes, including congestion of splenic blood vessels and sinusoids, suggesting increased vascularity within the organ. An increased number of melanomacrophage centers was also observed, reflecting enhanced phagocytic activity and activation of the fish immune response. Additionally, a noticeable expansion of the red pulp was evident, which may be associated with increased blood cell sequestration and immune cell infiltration while preserving the overall splenic structure.

The infected group **(G3)** exhibited severe pathological alterations characterized by marked depletion and reduction of the white pulp, indicating lymphoid tissue destruction and suppression of immune function as a consequence of bacterial infection. This lesion was accompanied by a pronounced expansion of the red pulp and a significant increase in melanomacrophage centers, suggesting intense phagocytic activity and the accumulation of cellular debris resulting from tissue injury and inflammation. These findings indicate that the bacterial challenge induced substantial disruption of the normal splenic architecture and impaired lymphoid integrity. In contrast, the infected group treated with bacteriophage **(G4)** showed considerable histological improvement compared with the untreated infected group. The white pulp remained prominent and well preserved, indicating recovery of the lymphoid tissue and restoration of normal splenic organization. The overall architecture of the spleen appeared closer to that of the control group, suggesting that bacteriophage treatment effectively mitigated the pathological effects of bacterial infection and contributed to maintaining splenic immune function. Overall, the histopathological findings demonstrate that bacterial infection caused significant alterations in splenic morphology, including white pulp depletion, red pulp expansion, and increased melanomacrophage accumulation, whereas bacteriophage treatment

markedly preserved the normal splenic architecture and reduced the severity of these pathological changes.

4. **Discussion**

The selection of *Streptococcus pyogenes* isolate RE13 as the host strain was based on its multidrug-resistant (MDR) phenotype, exhibiting resistance to 14 antibiotics, making it a suitable model for evaluating bacteriophage efficacy. Prophage induction under antibiotic stress (Fig. 1) confirmed that chemical agents effectively activate the bacterial SOS response and initiate the lytic cycle, consistent with the mechanism first described by Lwoff (1953).

Transmission Electron Microscopy (TEM) showed that the isolated phage possesses an icosahedral head (~62 nm) and a long non-contractile tail (~115 nm), characteristic features of the *Siphoviridae* family (class *Caudoviricetes*), in agreement with the classification proposed by Ackermann (2009). In addition, 16S rRNA sequencing and phylogenetic analysis (Fig. 2) demonstrated 100% identity between the hosts isolate and reference *S. pyogenes* strains, confirming its classification as Group A Streptococcus (GAS).

The isolated phage exhibited high stability under physiological conditions, maintaining infectivity at temperatures up to 40°C and at neutral pH (7.0), while losing activity under extreme temperatures and pH values, reflecting the sensitivity of its protein capsid structure. These findings are consistent with Jończyk et al. (2011), who reported that the stability of *Siphoviridae* phages is strongly influenced by environmental conditions. Similarly, complete inactivation following prolonged UV exposure highlights the susceptibility of phage DNA to radiation-induced damage.

Adsorption analysis (Fig. 7) demonstrated rapid attachment of the phage to the bacterial host, with phage titers decreasing from 9.98 to 6.00 log10 PFU/ml within a

few minutes, suggesting efficient recognition of conserved surface receptors. The one-step growth experiment (Fig. 8) revealed a short latent period of 15 min and a burst size of approximately 18.8 PFU/cell, followed by a secondary infection cycle after 60 min. These growth characteristics agree with the classical model of Ellis and Delbrück (1939) and indicate efficient phage replication, a desirable feature for therapeutic applications (Kropinski, 2024).

Moreover, the phage displayed a relatively broad lytic spectrum, lysing 25% of the tested clinical isolates, with strong (+++) lytic activity against eight MDR strains (Table 3). This broad host range suggests recognition of conserved bacterial receptors and supports its potential as a targeted antimicrobial agent that minimizes disruption of the normal microbiota, as previously discussed by Hyman and Abedon (2010).

The current data demonstrated that *S. pyogenes* infection induced marked hepatorenal dysfunction, oxidative stress, and immunosuppression in Nile tilapia, while treatment with its specific bacteriophage (SPB) effectively mitigated these adverse effects. The significant elevation in liver enzymes (ALT, AST, and ALP) observed in the infected group (G3) reflects hepatocellular damage and membrane leakage, which are common indicators of liver injury in fish under pathogenic stress. Similar findings have been widely reported in bacterial infections, where toxins and inflammatory responses disrupt hepatic integrity (Nidarshanaa and Krishnakumar, 2026; Aly et al., 2023; Farag et al., 2023; Janelidze et al., 2022; Abu-Elala et al., 2020; Saleh et al., 2024). The observed increase in creatinine and urea levels further confirms renal impairment, likely due to systemic infection and metabolic disturbances. Interestingly, treatment with SPB (G4) significantly reduced these elevated hepatorenal markers, indicating a protective and therapeutic role of

544 bacteriophages. This improvement may be attributed to the specific lytic activity of
545 SPB against *S. pyogenes*, leading to reduced bacterial load and subsequent alleviation
546 of tissue damage.

547 Oxidative stress plays a critical role in the pathogenesis of bacterial infections.
548 In the current study, the infected group exhibited a significant decline in antioxidant
549 parameters (TAC, SOD, CAT, and GSH), suggesting excessive production of reactive
550 oxygen species (ROS) and depletion of antioxidant defenses. This imbalance between
551 oxidants and antioxidants is a hallmark of cellular stress and damage (Rajashekaraiah
552 et al., 2021; Shohrati et al., 2025; Ferrari et al., 2024; Mohammed et al., 2023).

553 Administration of SPB significantly improved antioxidant status, as evidenced
554 by increased levels of TAC, SOD, CAT, and GSH in G4. This restoration may be
555 linked to reduced oxidative burden following bacterial clearance. Notably, the SPB-
556 only group (G2) showed the highest antioxidant levels, suggesting that bacteriophages
557 may exert a modulatory or stimulatory effect on antioxidant systems even in the
558 absence of infection as supported by. Choi et al., (2023); Zeng et al. (2025) ;
559 Preenanka et al., (2022)

560 Regarding immune response, the significant reduction in lysozyme and nitric
561 oxide levels in the infected group indicates suppression of innate immunity.
562 Lysozyme is a key antimicrobial enzyme (Ferraboschi et al., 2021), while nitric oxide
563 plays an essential role in pathogen defense. Their depletion reflects compromised
564 immune competence under infection (Roberts et al., 2024).Conversely; SPB treatment
565 enhanced these immunological parameters, indicating recovery of immune function.
566 This may be explained by the reduction of pathogen-induced immunosuppression and
567 possible immunomodulatory effects of bacteriophages (Criscuolo et al., 2017; Souza
568 et al., 2023; Sippel and Velimirov, 2026). Overall, the findings of this study highlight

569 the dual role of SPB as both an antimicrobial and a physiological modulator, capable
570 of alleviating infection-induced damage and restoring normal biological functions.
571 These results support the potential application of bacteriophage therapy as a
572 promising and eco-friendly alternative to antibiotics in aquaculture (Ferraboschi et
573 al., 2021; Roberts et al., 2024; Souza et al., 2023; Criscuolo et al., 2017).

574 The histopathological examination of the intestine, liver, and spleen
575 demonstrated the detrimental effects of *S. pyogenes* infection and the protective role
576 of bacteriophage therapy. The intestinal sections of the infected group (G3) revealed
577 severe pathological alterations, including mucosal sloughing, inflammatory cell
578 infiltration, and marked atrophy of the intestinal villi as a result of enteritis. In
579 contrast, the infected group treated with bacteriophage (G4) showed preserved
580 intestinal architecture, with intact villi and increased goblet cell activity, indicating
581 enhanced mucosal protection and regeneration. These findings are in agreement with
582 Mohammed et al. (2023), who reported similar improvements in intestinal integrity
583 following bacteriophage treatment.

584 The liver in the infected group (G3) demonstrated marked vacuolar fatty
585 degeneration of hepatocytes, a characteristic lesion associated with streptococcal
586 septicemia. These findings are consistent with the observations of Abu-Elala et al.
587 (2020), who suggested that streptococcal toxins directly damage hepatic parenchymal
588 cells, resulting in cellular degeneration and impaired liver function. Conversely, the
589 infected group treated with bacteriophage (G4) exhibited a remarkable restoration of
590 hepatocyte morphology and a significant reduction in degenerative changes. These
591 results are consistent with those reported by Preenanka et al. (2022), who attributed
592 hepatic recovery to the rapid elimination of bacterial pathogens from the hepatic

portal circulation, thereby reducing the toxic burden on liver tissue and facilitating tissue regeneration.

Similarly, the spleen of the infected group (G3) showed marked vascular congestion and a pronounced increase in melanomacrophage centers, accompanied by depletion of the white pulp, reflecting an intense inflammatory response and activation of the splenic phagocytic system. These observations agree with the findings of Abu-Elala et al. (2020) and Mohammed et al. (2023). In contrast, bacteriophage treatment in the infected group (G4) markedly preserved the white pulp architecture and reduced splenic congestion, indicating attenuation of tissue damage and maintenance of splenic immune function. These findings support the results of Ferrari et al. (2024), who proposed that bacteriophages exert immunomodulatory effects by selectively eliminating bacterial pathogens without inducing the excessive inflammatory responses that typically disrupt splenic architecture.

Conclusion

The findings of the present study demonstrate that the induced bacteriophage SPB is a promising and safe biocontrol agent against multidrug-resistant (MDR) *S. pyogenes*. Comprehensive characterization by phylogenetic analysis, transmission electron microscopy, physicochemical evaluation, and whole genome sequencing confirmed its classification within the *Siphoviridae* family, high environmental stability, lytic potential, and the absence of virulence-associated genes, supporting its suitability for therapeutic applications. Both in vitro and *in-vivo* investigations confirmed the strong antibacterial activity of SPB against MDR *S. pyogenes*. In the Nile tilapia experimental model, phage therapy significantly increased survival rates and effectively mitigated the pathological consequences of bacterial infection by

improving hepatorenal function, enhancing innate immune responses through elevated nitric oxide and lysozyme activities, and restoring antioxidant defense mechanisms. Moreover, histopathological examination revealed marked recovery of liver, kidney, and spleen tissues, with reduced inflammatory reactions and bacterial-induced lesions compared with untreated infected fish. Taken together, these results highlight the considerable potential of SPB as an environmentally friendly and effective alternative to conventional antibiotics for the management of *S. pyogenes* infections. The study provides valuable evidence supporting the application of bacteriophage therapy as a sustainable strategy to combat antimicrobial resistance and improve disease control in aquaculture. Future investigations should focus on large-scale field trials, optimization of phage formulations and delivery systems, and evaluation of long-term efficacy and safety to facilitate the practical implementation of phage-based therapeutics.

Figure legend

Figure 1: Prophage induction from *S. pyogenes* using antibiotic stress.

Figure3: Transmission electron micrograph (TEM) of the purified phage negatively stained with 2% uranyl acetate.

Figure 2: Phylogenetic tree showing the evolutionary relationship of *Streptococcus pyogenes* strain RE13 (PX884326.1) based on 16S rRNA gene sequences

Figure 4: Thermal stability profile of the isolated phage.

Figure 5: pH stability profile of phage.

Figure 6: Effect of UV radiation on the viability of phage.

Figure 7: Adsorption rate of Phage.

Figure 8: One-step growth curve of Phage.

Figure 9: Gross pathological changes in experimentally infected Nile tilapia (*Oreochromis niloticus*) with *S. pyogenes*. (A) External lesions including focal scales

642 detachment (black arrows) and hemorrhages and caudal and dorsal fin erosion (red
643 arrows). (B) Enlarged dark and congested gall bladder (blue arrow). (C) Visceral
644 organs congestion and hemorrhagic lesions. (D) Gill rot (black arrow) associated with
645 enlarged gall bladder (blue arrow).

646 **Figure 10**: Histopathological examination of intestinal sections stained with
647 hematoxylin and eosin (H&E) revealed distinct histological changes among the
648 experimental groups. The phage-treated group (G2) showed mild degeneration (D)
649 and an increase in the thickness of the muscular layer (M). In contrast, the infected
650 group (G3) exhibited severe degeneration (D) and necrosis (N), resulting in marked
651 villous sloughing. The normal control group (G1) displayed normal intestinal
652 architecture with prominent goblet cells (G). Meanwhile, the infected group treated
653 with bacteriophage (G4) showed restoration of intestinal tissue integrity, characterized
654 by an increased number of goblet cells (G) and improved mucosal structure compared
655 with the infected untreated group.

656 **Figure 11 B:** Mean intestinal villi length and width (µm) in the experimental groups.
657 Bars represent the mean values of intestinal villi length and width for G1, G2, G3, and
658 G4.

659 **Figure11 A:** Histopathological intestinal sections stained with hematoxylin and eosin
660 (H&E, 10×) showing the villus length and width in the examined groups. The infected
661 group (G3) exhibited marked villous atrophy and sloughing. In contrast, the infected
662 group treated with bacteriophage (G4) showed restoration of the intestinal tissue
663 architecture, with increased mucosal folding and improved villous structure,
664 appearing nearly comparable to that of the normal control group (G1).

665 **Figure 12:** Histopathological sections of the liver and pancreas stained with
666 hematoxylin and eosin (H&E) revealed various histopathological alterations among

the examined groups. The phage-treated group (G2) showed degeneration of hepatic cells and pancreatic tissue (D), along with congestion and dilation of the hepatic vein (Co). The infected group (G3) exhibited marked congestion and dilation of the hepatic vein (Co) and hepatic sinusoids (arrow), degeneration of pancreatic tissue (D), and fatty degeneration of hepatocytes (Fd) accompanied by pyknotic nuclei (P). The control group (G1) and the infected group treated with bacteriophage (G4) showed congested blood vessels (Co) and moderate degeneration of hepatic cells and pancreatic tissue (D).

Figure 13: Histopathological sections of the spleen stained with hematoxylin and eosin (H&E) revealed distinct histological changes among the experimental groups. The phage-treated group (G2) showed blood congestion (Co), increased numbers of melanomacrophages (Hs), and an expansion of the red pulp (R). The infected group (G3) exhibited depletion of the white pulp (W), accompanied by an increase in the red pulp (R) and melanomacrophages (Hs). In contrast, the control group (G1) and the infected group treated with bacteriophage (G4) showed prominent white pulp (W), indicating a relatively preserved splenic architecture.

Tables

Table 1: Antibiotic Resistance Profiles of Selected *S. pyogenes* Clinical Isolates.

Table 2: Morphological and Biochemical Characteristics of *S. pyogenes* Isolates.

Table 3: Host Range of Phage against all isolate

Table 4: Effect of *S.pyogenes* and\or *S.pyogenes* bacteriophage (SPB) on the hepatorenal functions of Nile tilapia after 5 days treatment.

Table 5: Effect of *S.pyogenes* and\or *S.pyogenes* bacteriophage (SPB) on the antioxidant and immunological parameters of Nile tilapia after 5 days treatment.

Ethics and consent to participate

The experiment was carried out in compliance with the rules established by the local committee for the care of experimental animals. The experimental protocol was approved by the Ethics of the Institutional Animal Care and Use Committee of Zagazig University, Egypt. The experimental procedures were conducted by following the NIH general guidelines for the Care and Use of Laboratory Animals in scientific investigations (ZU-IACUC/1/F/232/2025). The fish were transported in plastic bags to the Wet Lab at Zagazig University's Department of Aquatic Animal Medicine in Egypt from Al-Abbassa Fish Hatchery in Sharkia Governorate, Egyptian permission from owners.

Credit authorship contribution statement

Alshimaa A.Khalil: Writing – review & editing, Supervision, Methodology, Investigation, Data curation, Conceptualization, Validation, and Investigation. Enas A. Ramadan: Writing – review & editing. Rewan Abdelaziz : Conceptualization, Writing – review & editing, Validation, Methodology, Investigation, Data curation. Rania Ali, Kasim Sakran Abass: Writing – review & editing, Visualization.

Declaration

Competing interest

The authors declare no conflict of interest.

Data availability statement

Availability of data and materials supporting the findings of this study are available upon reasonable request from the corresponding author.

Consent to Publish declaration

Not applicable.

Funding

No funding

Acknowledgment

The authors thank their respected universities.

References

1. Ackermann, H. W. (2011). *Bacteriophage Taxonomy: An Overview.* Methods in Molecular Biology, 681, 3-10.
2. Ackermann, H. W. (2009). Phage classification and characterization. *Methods in Molecular Biology*, 501, 127-140.
3. Ellis, E. L., & Delbrück, M. (1939). The growth of bacteriophage. *The Journal of General Physiology*, 22(3), 365.
4. Jończyk, E., et al. (2011). The influence of external factors on bacteriophages—review. *Folia Microbiologica*, 56, 191-200.
5. Efstratiou, A., & Lamagni, T. (2021). *The Global Challenge of Group A Streptococcal Diseases.* The Lancet Infectious Diseases.
6. Gordillo Altamirano, F. L., & Barr, J. J. (2021). *Phage Therapy in the Post-Antibiotic Era.* Clinical Microbiology Reviews, 32(2).
7. Joerger, R. D. (2020). *Environmental Stability of Bacteriophages: pH, Temperature, and UV Stress.* Virology Journal, 17(1).
8. Sullivan, M., & Lehman, S. (2021). *Histopathological Evaluation of Phage-Induced Tissue Recovery in Aquatic Models.* Fish & Shellfish Immunology, 112.
9. Walker, Mark J.; Barnett, Timothy C.; Fordyce, Euan K.; Cave, Mary E.; Mesnage, Stéphane; Knight, David R.; Letellier, Anick; Steele-Mortimer, Olivia; Nizet, Victor. (2022). *Disease Manifestations and Pathogenic*

744 *Mechanisms of Streptococcus pyogenes*. Nature Reviews Microbiology,
745 20(6), 335-349.
746 10. Ackermann, H. W. (2009). *Basic phage electron microscopy.* Methods in
747 Molecular Biology, 501, 113-126.
748 11. Arndt, David; Grant, Jason R.; Marcu, Ana; Sajed, Tanvir; Pon, pon; Liang,
749 Yannick; Wishart, David S. (2016). PHASTER: a better, faster version of the
750 PHAST phage search tool. Nucleic Acids Research, 44(W1), W16-W21.
751 12. Aziz, Ramy K.; Bartels, Detlef; Best, Aaron A.; DeJongh, Matthew; Disz,
752 Terrence; Edwards, Robert A.; Formsma, Kevin; Gerdes, Svetlana; Glass,
753 Elizabeth M.; Kubal, Michael; Meyer, Folker; Olsen, Gary J.; Olson, Robert;
754 Osterman, Andrei L.; Overbeek, Ross A.; McNeil, Leslie S.; Paarmann,
755 Daniel; Paczian, Tobias; Parrello, Bruce; Pusch, Gordon D.; Reich, Claudia;
756 Stevens, Rick; Vassieva, Olga; Vonstein, Veronika; Wilke, Andreas;
757 Zagnitko, Olga. (2008). The RAST Server: rapid annotations using
758 subsystems technology. BMC Genomics, 9(1), 75.
759 13. Clokie, J. J., & Kropinski, A. M. (2009). *Bacteriophages: Methods and*
760 *Protocols.* Humana Press.
761 14. Garrity, George M.; Brenner, Don J.; Krieg, Noel R.; Staley, James T. (2005).
762 *Bergey's Manual of Systematic Bacteriology.* Springer.
763 15. Kropinski, Andrew M.; Mazzocco, Amanda; Waddell, Thomas E.; Lingohr,
764 Erika; Johnson, Roger P. (2009). Enumeration of bacteriophages by double-
765 layer agar plaque assay. Methods in Molecular Biology, 501, 69-76.
766 16. Kumar, Sudhir; Stecher, Glen; Li, Michael; Knyaz, Christina; Tamura,
767 Koichiro. (2018). MEGA X: Molecular Evolutionary Genetics Analysis
768 across Computing Platforms. Molecular Biology and Evolution, 35(6), 1547.

17. Sillankorva, Sanna; Neubauer, Peter; Azeredo, Joana. (2008). Physicochemical characterization of *a Pseudomonas fluorescens* phage. Letters in Applied. Microbiology, 46(1), 28-33.
18. Hyman, P., & Abedon, S. T. (2010). "Bacteriophage host range and bacterial resistance." *Advances in Applied Microbiology*, 70, 217-248.
19. Kropinski, A. M. (2024). "Practical Aspects of Bacteriophage Adsorption and One-Step Growth Curves." *Methods in Molecular Biology*, vol. 2731.
20. Suvarna, S. Kim; Layton, Christopher; Bancroft, John D. (2018). Bancroft's Theory and Practice of Histological Techniques. Elsevier.
21. Tan, Ronghui; Chen, Libin; Li, Xiaoting; Zhang, Yanni; Wang, Jing; Wang, Ziqing; Liu, Sijia; He, Yang. (2022). Therapeutic efficacy of phages in aquatic models. Aquaculture Research, 53(4), 1120-1135.
22. Weisburg, William G.; Barns, Susan M.; Pelletier, Dale A.; Lane, David J. (1991). 16S ribosomal DNA amplification for phylogenetic study. Journal of Bacteriology, 173(2), 697-703.
23. Clinical and Laboratory Standards Institute (CLSI). (2023). *Performance Standards for Antimicrobial Susceptibility Testing*. 33rd ed. CLSI supplement M100. Wayne, PA: Clinical and Laboratory Standards Institute.
24. Lwoff, A. (1953). Lysogeny. Bacteriological Reviews, 17(4), 269.
25. Sahoo DM, Rukmini R. Quantitative analysis of serum levels of alanine and aspartate aminotransferases, γ-Glutamyl transferase and alkaline phospatase as predictor of liver diseases. Am inter J res in form. Appl Nat Sci. 2014; (9) 51–55.
26. Coulombe J, Favreau L. A new simple semimicro method for colorimetric determination of urea. Clin. Chem. 1963; (9) 102-108.

794 27. Larsen K. Creatinine assay by a reaction-kinetic principle. Clin. Chim. Acta
795 1972; (41) 209–217.
796 28. Aebi H. Catalase in vitro. Methods Enzymol. 1984; (105) 121-6.
797 29. Nishikimi M, Rao NA, Yagi K. The occurrence of superoxide anion in the
798 reaction of reduced phenazine methosulfate and molecular oxygen.
799 Biochemical and Biophysical Research Communications 1972; (2) 849-854.
800 30. Beutler E, Duron O, Kelly BM. Improved method for the determination of
801 blood glutathione. J of Lab and Clin Medicine. 1963;(61) 882-888.
802 31. Ellis AE. Lysozyme assays, In: J.S. Stolen, T.C. Fletcher, D.P. Anderson,
803 B.S. Roberson, W.B. Van Muiswinkel (Eds.), Techniques in Fish
804 Immunology,NJ: SOS Publications,Fair Haven, pp. 1990; 101-103.
805 32. Montgomery H, Dymock JF. The determination of nitrite in water. The
806 Analyst, 1961; (102) 414-416.
807 33. Bancroft JD, Layton C, Suvarna SK. Bancroft's theory and practice of
808 histological techniques. Churchill Livingstone Elsevier. 2013.
809 34. Stevens JP. Intermediate statistics: A modern approach. Oxfordshire,
810 England, UK: Routledge. 2013.
811 35. Kwikiriza, G., Muthoka, M., Omara, T., Abaho, I., Tibihika, P.D., Curto, M.,
812 Opiyo, M.A., Munguti, J., Abwao, J., Orina, P. and Meimberg, H. (2025),
813 Nile Tilapia (Oreochromis niloticus L.) Cage Aquaculture in Africa: Potential
814 Threats to Congeneric Fish Species and Advances to Detect Escapes. Aqua.
815 Fish & Fisheries, 5: e70090. https://doi.org/10.1002/aff2.70090
816 36. Kim, J. H., Gomez, D. K., Choresca Jr, C. H., & Park, S. C. (2007). Detection
817 of major bacterial and viral pathogens in trash fish used to feed cultured
818 flounder in Korea. Aquaculture, 272(1-4), 105-110.

819 37. Abou El-Gheit, E. S. N. (2005). Streptococcus infections among farmed and
820 wild tilapia fish in Egypt. The Egyptian Journal of Experimental Biology
821 (Zoology), 1, 1-7.
822 38. Gundi, V. A. K. B., Bogireddy, D., Vundru, A. K., Arthala, P. K., Vadela, M.
823 B., Karri, S., .Kodali, V. P. (2025). Microbial pathogens in aquaculture: a
824 review of emerging threats. Academia Biology, 3(3).
825 https://doi.org/10.20935/AcadBiol7814
826 39. Abdallah ESH, Metwally WGM, Abdel-Rahman MAM, Albano M,
827 Mahmoud MM. Streptococcus agalactiae Infection in Nile Tilapia
828 (Oreochromis niloticus): A Review. Biology (Basel). 2024 Nov
829 11;13(11):914. doi: 10.3390/biology13110914. PMID: 39596869; PMCID:
830 PMC11591708.
831 40. David B. Olawade, Oluwaseun Fapohunda, Eghosasere Egbon, Oladipo A.
832 Ebiesuwa, Sunday Oluwadamilola Usman, Alaba O. Faronbi, Sandra Chinaza
833 Fidelis, Phage therapy: A targeted approach to overcoming antibiotic
834 resistance, Microbial Pathogenesis, Volume 197, 2024, 107088, ISSN 0882-
835 4010,https://doi.org/10.1016/j.micpath.2024.107088.(https://www.sciencedire
836 ct.com/science/article/pii/S0882401024005552)
837 41. da Paz, C. A., B. M. P. A. da Costa, M. K. O. Hamoy, M. F. d. Santos, L. L.
838 da Rocha, Y. d. S. Deiga, A. d. S. Barbosa, A. L. G. do Amaral, T. M.
839 Câmara, G. B. Barbosa, D. B. de Araujo, P. F. P. Hartcopff, L. A. L. Barbas,
840 N. A. Muto, M. Hamoy. Establishing a safe anesthesia concentration window
841 for *Nile tilapia* (*Oreochromis niloticus*) (Linnaeus 1758) by monitoring
842 cardiac activity in eugenol immersion baths, Comparative Biochemistry and
843 Physiology Part C: Toxicology & Pharmacology, Volume 278, 2024, 109839,

844 ISSN 1532-0456, https://doi.org/10.1016/j.cbpc.2024.109839.
845 (https://www.sciencedirect.com/science/article/pii/S1532045624000073)
846 42. Janelidze N, Jaiani E, Didebulidze E, Kusradze I, Kotorashvili A, Chalidze K,
847 Porchkhidze K, Khukhunashvili T, Tsertsvadze G, Jgenti D, et al. Phenotypic
848 and Genetic Characterization of Aeromonas hydrophila Phage AhMtk13a and
849 Evaluation of Its Therapeutic Potential on Simulated Aeromonas Infection
850 in *Danio rerio. Viruses*. 2022; 14(2):412. https://doi.org/10.3390/v14020412
851 43. Nidarshanaa S., Krishnakumar V. (2026): Role of nanotechnology in
852 aquaculture disease management: A comparative review, Aquaculture and
853 Fisheries. ISSN 2468-550X, https://doi.org/10.1016/j.aaf.2025.12.012.
854 44. Aly, S. M., A. E. Eissa, N. Abdel-Razek, A. O. El-Ramlawy, The
855 antibacterial activity and immunomodulatory effect of naturally synthesized
856 chitosan and silver nanoparticles against *Pseudomonas fluorescence* infection
857 in Nile tilapia (*Oreochromis niloticus*): An in vivo study, Fish & Shellfish
858 Immunology, Volume 135, 2023, 108628, ISSN 1050-4648,
859 https://doi.org/10.1016/j.fsi.2023.108628.
860 45. Farag, M.R.; Abo-Al-Ela, H.G.; Alagawany, M.; Azzam, M.M.; El-Saadony,
861 M.T.; Rea, S.; Di Cerbo, A.; Nouh, D.S. Effect of Quercetin Nanoparticles on
862 Hepatic and Intestinal Enzymes and Stress-Related Genes in Nile Tilapia Fish
863 Exposed to Silver
864 Nanoparticles. *Biomedicines* 2023, *11*,663.https://doi.org/10.3390/biomedicin
865 es11030663
866 46. Saleh, A.A.; Mohamed, A.Z.; Elnesr, S.S.; Khafaga, A.F.; Elwan, H.; Abdel-
867 Aziz, M.F.; Khaled, A.A.; Hafez, E.E. Expression and Immune Response
868 Profiles in Nile Tilapia (*Oreochromis niloticus*) and European Sea Bass

(*Dicentrarchus labrax*) During Pathogen Challenge and Infection. *Int. J. Mol. Sci.* **2024**, *25*, 12829. https://doi.org/10.3390/ijms252312829

47. Abu-Elala N.M.,Abd-Elsalam R.M., Younis N. A. Streptococcosis, Lactococcosis and Enterococcosis are potential threats facing cultured Nile tilapia (Oreochomis niloticus) production, Aquaculture Research. 2020; 51:4183–4195
48. Ferrari, N.A.; Favero, L.M.; Facimoto, C.T.; Dall Agnol, A.M.; Gaeta, M.L.; de Oliveira, T.E.S.; Gonçalves, D.D.; Lopera-Barrero, N.M.; Pereira, U.d.P.; Di Santis, G.W. Clinical and Histopathological Evolution of Acute Intraperitoneal Infection by Streptococcus agalactiae Serotypes Ib and III in Nile Tilapia. Fishes 2024, 9, 279.
49. Mohammed R. S., Wassif I. M., and Tahoun E. Histopathological Lesions of Some Microbial Infections in Tilapia Fish at El Salam Canal, Egypt Damanhour Journal of Veterinary Sciences 9 (1), (2023) 23-22
50. Preenanka R., Safeena M. P., Krishnan R. ,2022. Evaluation of therapeutic potential of Streptococcus phage-1A against Streptococcus agalactiae infection in Nile tilapia (Oreochromis niloticus) Aquaculture International https://doi.org/10.1007/s10499-022-01036-w
51. Rajashekaraiah, V., Hsieh, C., & Pallavi, M. (2021). Modulations in Oxidative Stress of Erythrocytes during Bacterial and Viral Infections. In Erythrocyte - A Peripheral Biomarker For Infection and Inflammation. Intech-Open. https://doi.org/10.5772/intechopen.98236
52. Shohrati M., Jafari M., Sadrzadeh M., Ebrahiminezhad H., Ghanei M. Severity-related differences on response of antioxidant defense system in

COVID-19 patients // Russian Journal of Infection and Immunity. - 2025. - Vol. 15. - N. 5. - P. 899-905. doi: 10.15789/2220-7619-SRD-17819

53. Choi Y, Hosseindoust A, Ha SH, Kim J, Min Y, Jeong Y, Mun J, Sa S, Kim J. Effects of dietary supplementation of bacteriophage cocktail on health status of weanling pigs in a non-sanitary environment. J Anim Sci Biotechnol. 2023 May 8;14(1):64. doi: 10.1186/s40104-023-00869-6. PMID: 37150809; PMCID: PMC10165815.

54. Ferraboschi P, Ciceri S, Grisenti P. Applications of Lysozyme, an Innate Immune Defense Factor, as an Alternative Antibiotic. Antibiotics (Basel). 2021 Dec 14;10(12):1534. doi: 10.3390/antibiotics10121534. PMID: 34943746; PMCID: PMC8698798.

55. Zeng, C., Qi, L., Guan, C.-L., Chang, Y.-L., He, Y.-Y., Zhao, H.-Z., Wang, C., Zhao, Y.-R., Dong, Y.-C., & Zhong, G.-F. (2025). Phage Therapy Enhances Survival, Immune Response, and Metabolic Resilience in Pacific White Shrimp (*Litopenaeus vannamei*) Challenged with *Vibrio parahaemolyticus*. *Fishes*, *10*(8), 366. https://doi.org/10.3390/fishes10080366

56. Roberts, J. M., Milo, S., & Metcalf, D. G. (2024). Harnessing the Power of Our Immune System: The Antimicrobial and Antibiofilm Properties of Nitric Oxide. *Microorganisms*, *12*(12), 2543. https://doi.org/10.3390/microorganisms12122543

57. Souza EB, Pinto AR, Fongaro G. Bacteriophages as Potential Clinical Immune Modulators. Microorganisms. 2023 Sep 1;11(9):2222. doi: 10.3390/microorganisms11092222. PMID: 37764066; PMCID: PMC10535580.

58. Sippel, K., & Velimirov, B. (2026). Phage Therapy: Application and Related Problems-A Review. *Life*, *16*(1), 57. https://doi.org/10.3390/life16010057

59. Criscuolo E, Spadini S, Lamanna J, Ferro M, Burioni R. Bacteriophages and Their Immunological Applications against Infectious Threats. J Immunol Res. 2017;2017:3780697. doi: 10.1155/2017/3780697. Epub 2017 Apr 16. PMID: 28484722; PMCID: PMC5412166.

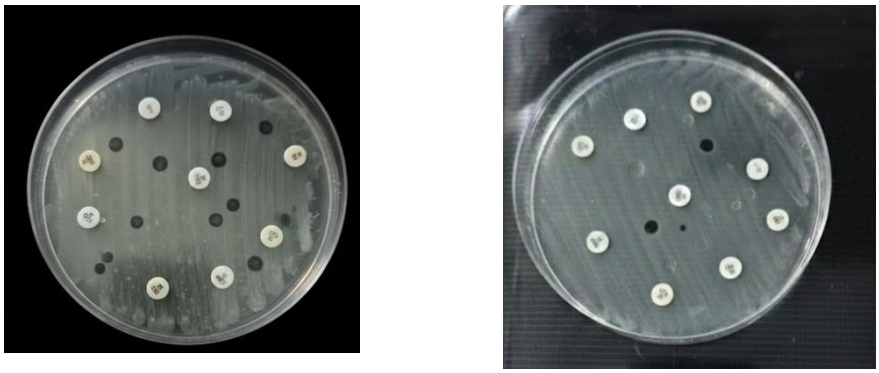


Figure 1: Prophage induction from *S. pyogenes* using antibiotic stress.

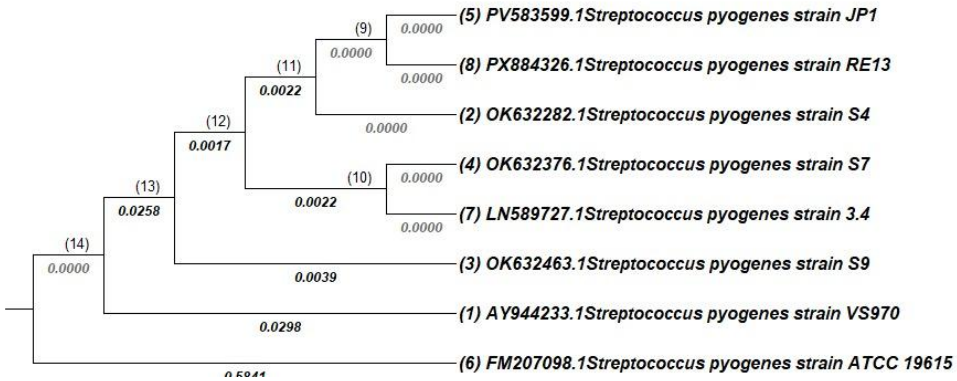


Figure 2: Phylogenetic tree showing the evolutionary relationship of *Streptococcus pyogenes* strain RE13 (PX884326.1) based on 16S rRNA gene sequences.

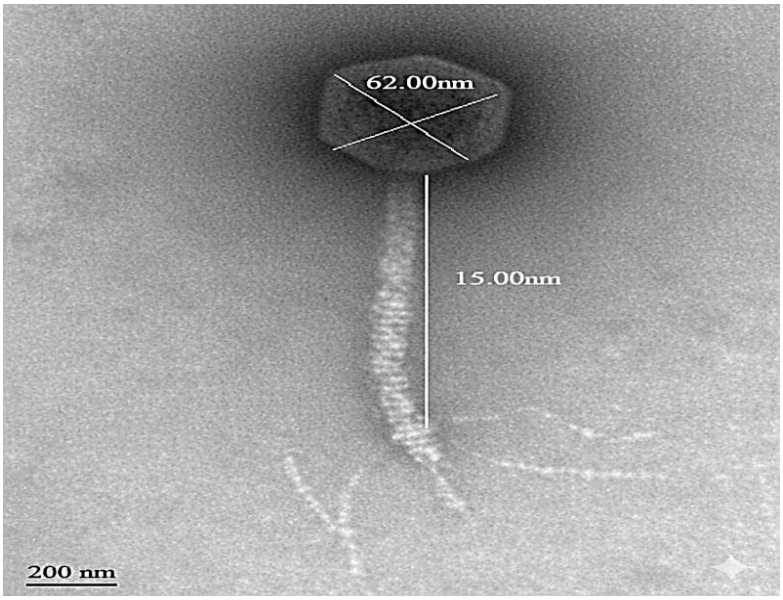


Figure3: Transmission electron micrograph (TEM) of the purified phage $\phi negatively stained with 2% uranyl acetate.

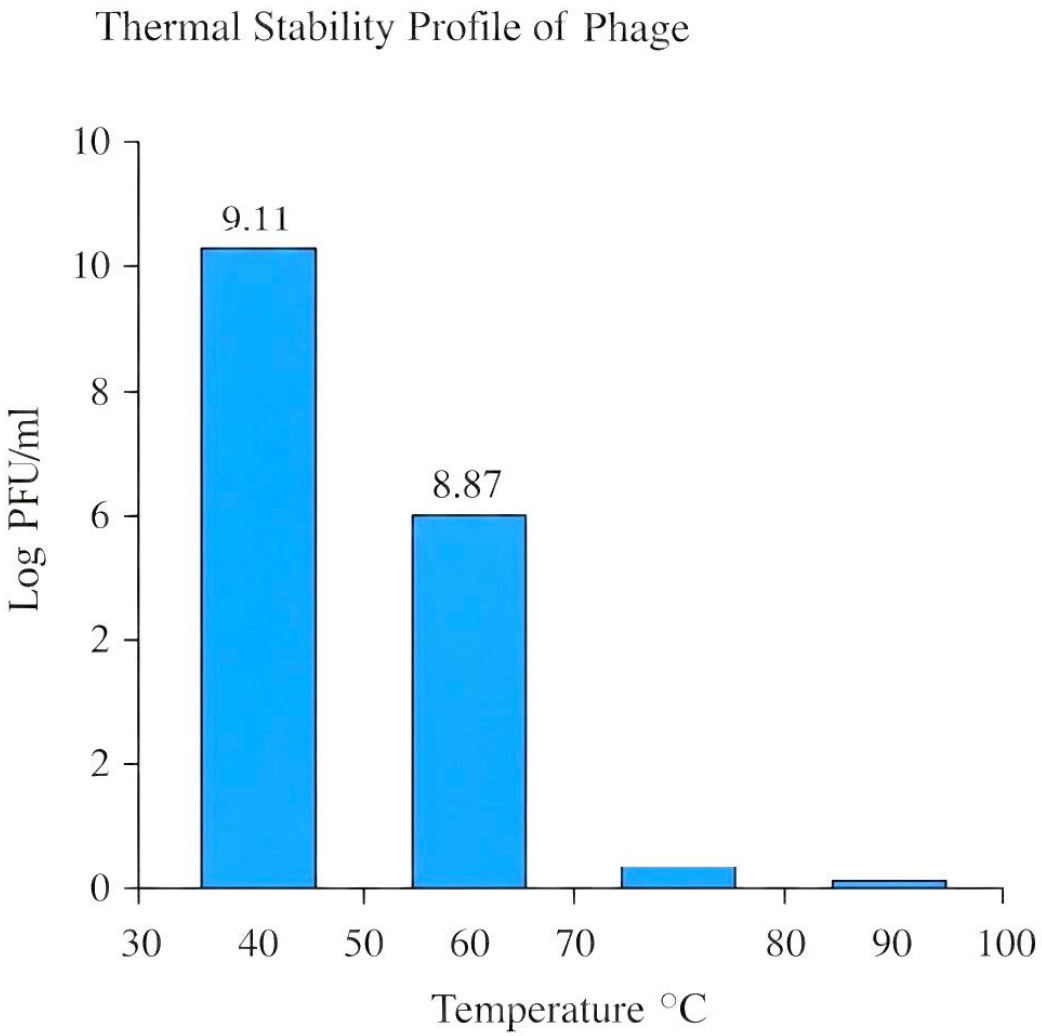


Figure 4: Thermal stability profile of the isolated phage.

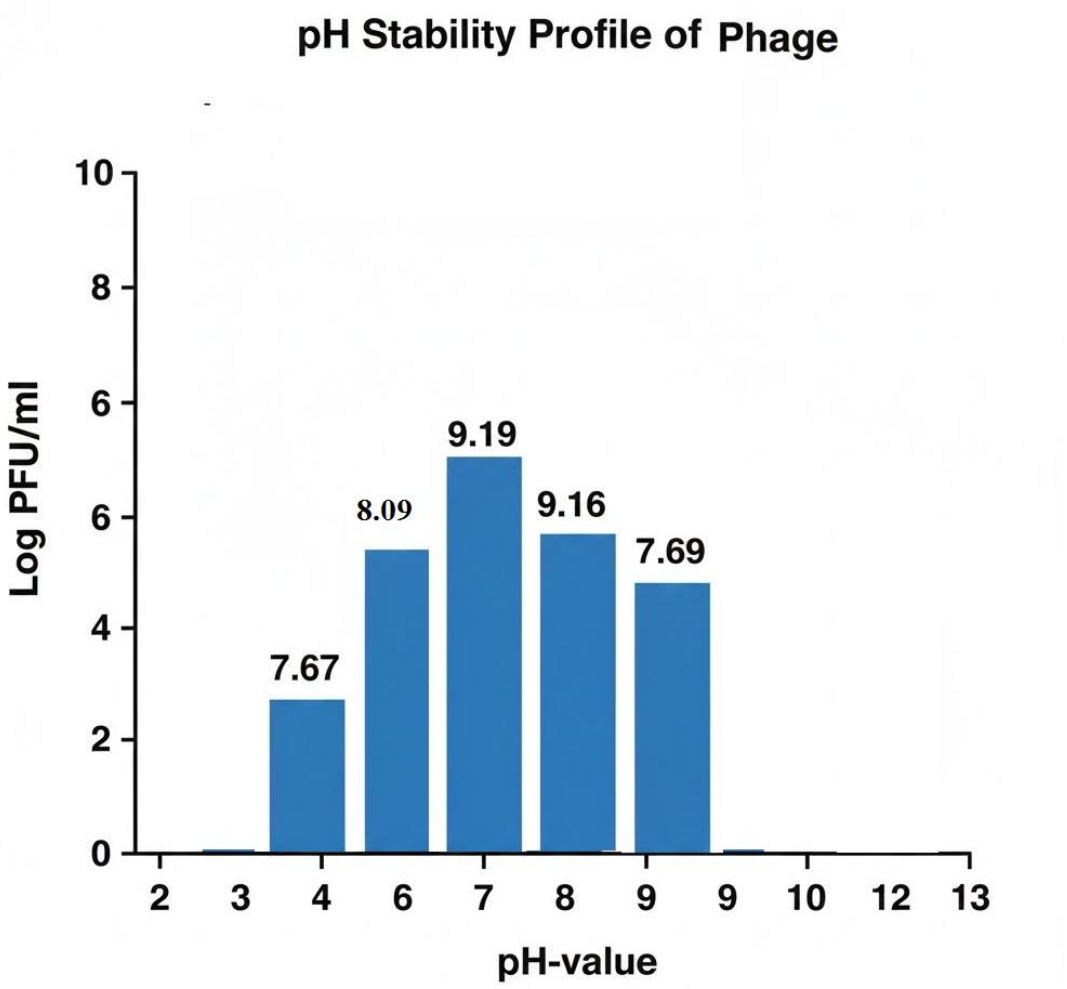


Figure 5: pH stability profile of phage.

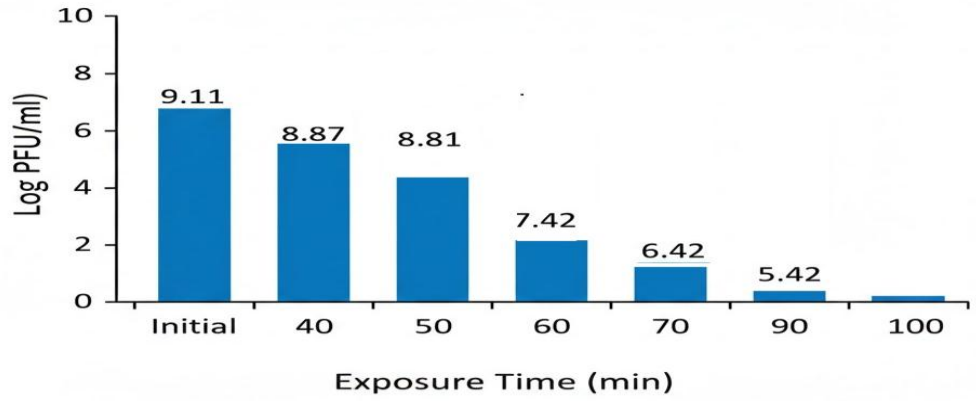


Figure 6: Effect of UV radiation on the viability of phage.

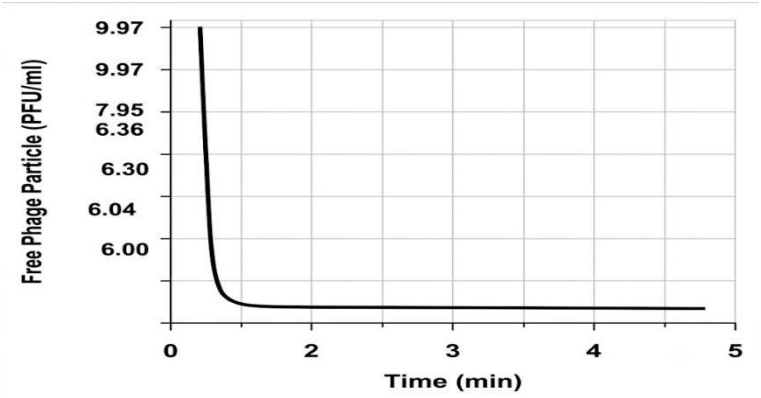


Figure 7: Adsorption rate of Phage**.**

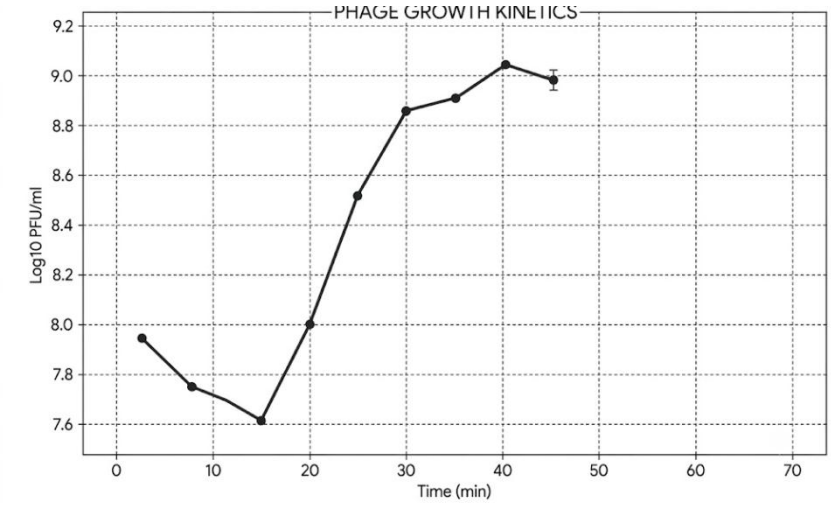


Figure 8: One-step growth curve of Phage

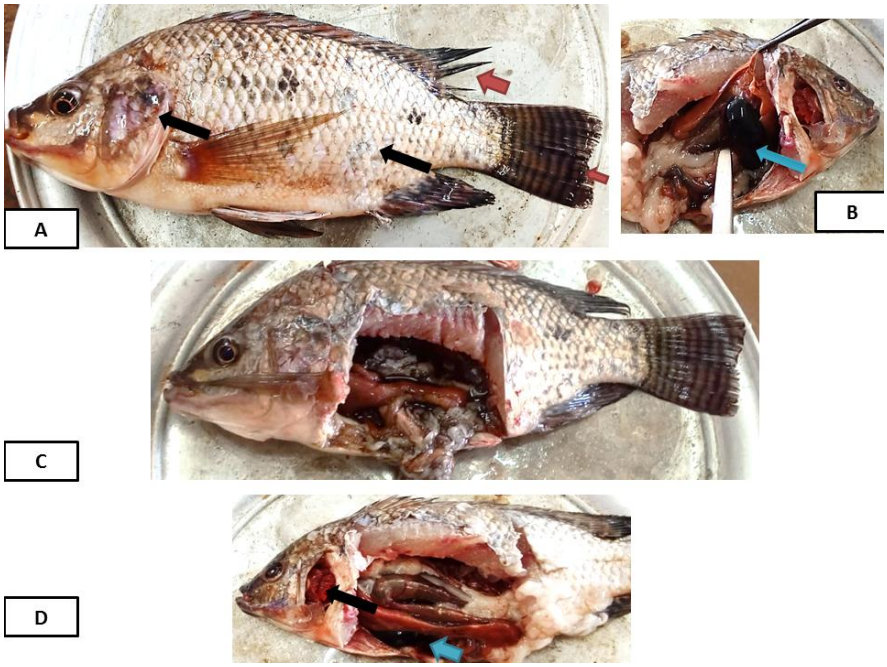


Figure 9. Gross pathological changes in experimentally infected Nile tilapia (*Oreochromis niloticus*) with *S. pyogenes*. (A) External lesions including focal scales detachment (black arrows) and hemorrhages and caudal and dorsal fin erosion (red arrows). (B) Enlarged dark and congested gall bladder (blue arrow). (C) Visceral organs congestion and hemorrhagic lesions. (D) Gill rot (black arrow) associated with enlarged gall bladder (blue arrow).

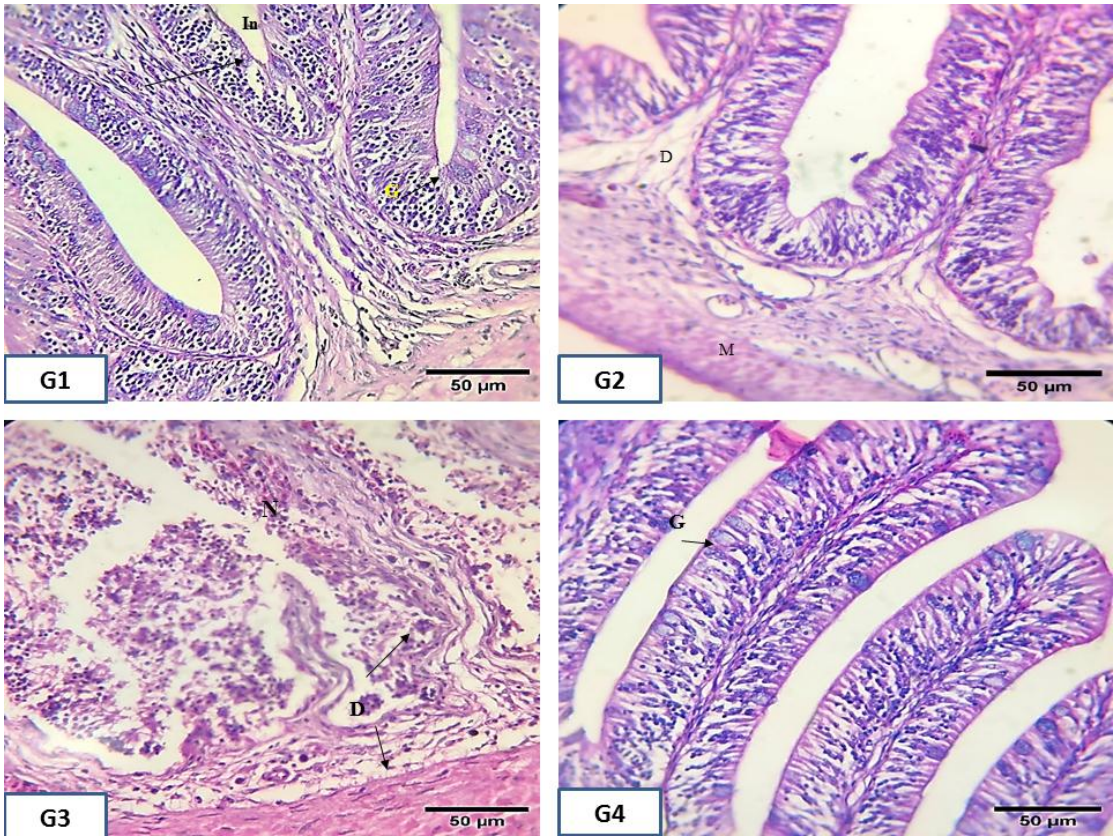


Figure 10. Histopathological examination of intestinal sections stained with hematoxylin and eosin (H&E) revealed distinct histological changes among the experimental groups. The phage-treated group (G2) showed mild degeneration (D) and an increase in the thickness of

the muscular layer (M). In contrast, the infected group (G3) exhibited severe degeneration (D) and necrosis (N), resulting in marked villous sloughing. The normal control group (G1) displayed normal intestinal architecture with prominent goblet cells (G). Meanwhile, the infected group treated with bacteriophage (G4) showed restoration of intestinal tissue integrity, characterized by an increased number of goblet cells (G) and improved mucosal structure compared with the infected untreated group.

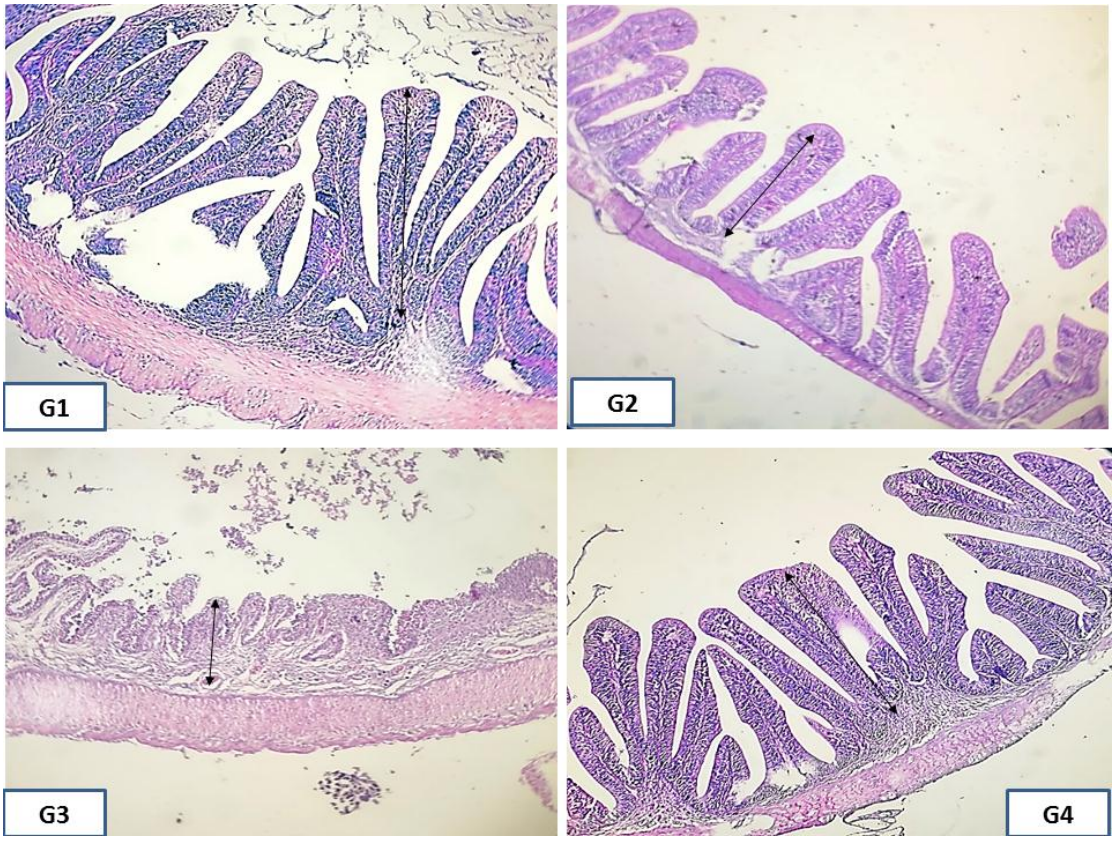


Figure11 A. Histopathological intestinal sections stained with hematoxylin and eosin (H&E, 10×) showing the villus length and width in the examined groups. The infected group (G3) exhibited marked villous atrophy and sloughing. In contrast, the infected group treated with bacteriophage (G4) showed restoration of the intestinal tissue architecture, with increased mucosal folding and improved villous structure, appearing nearly comparable to that of the normal control group (G1).

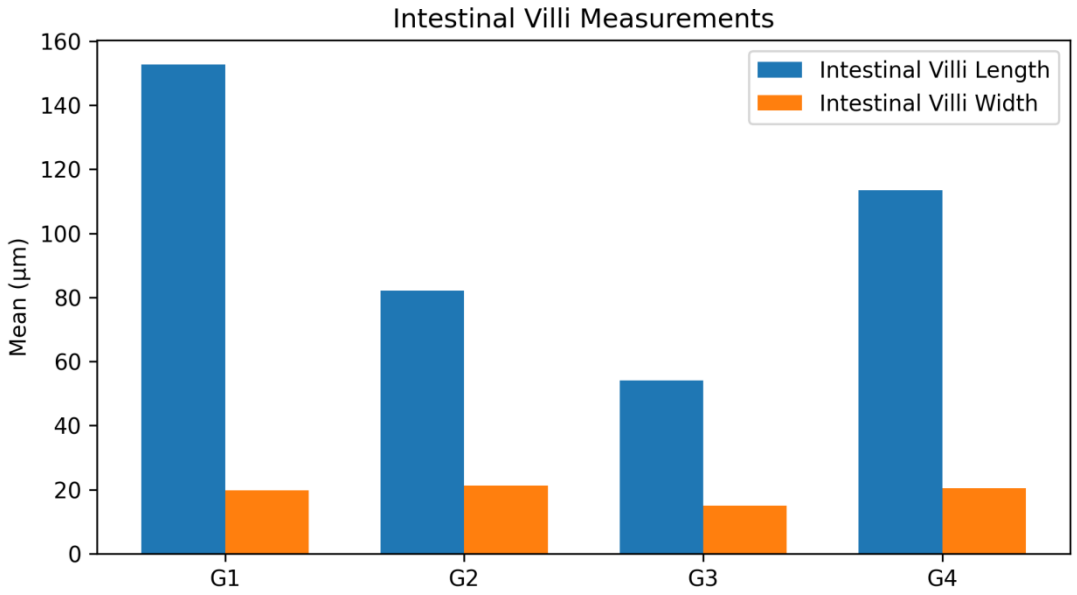


Figure 11 B. Mean intestinal villi length and width (µm) in the experimental groups. Bars represent the mean values of intestinal villi length and width for G1, G2, G3, and G4.

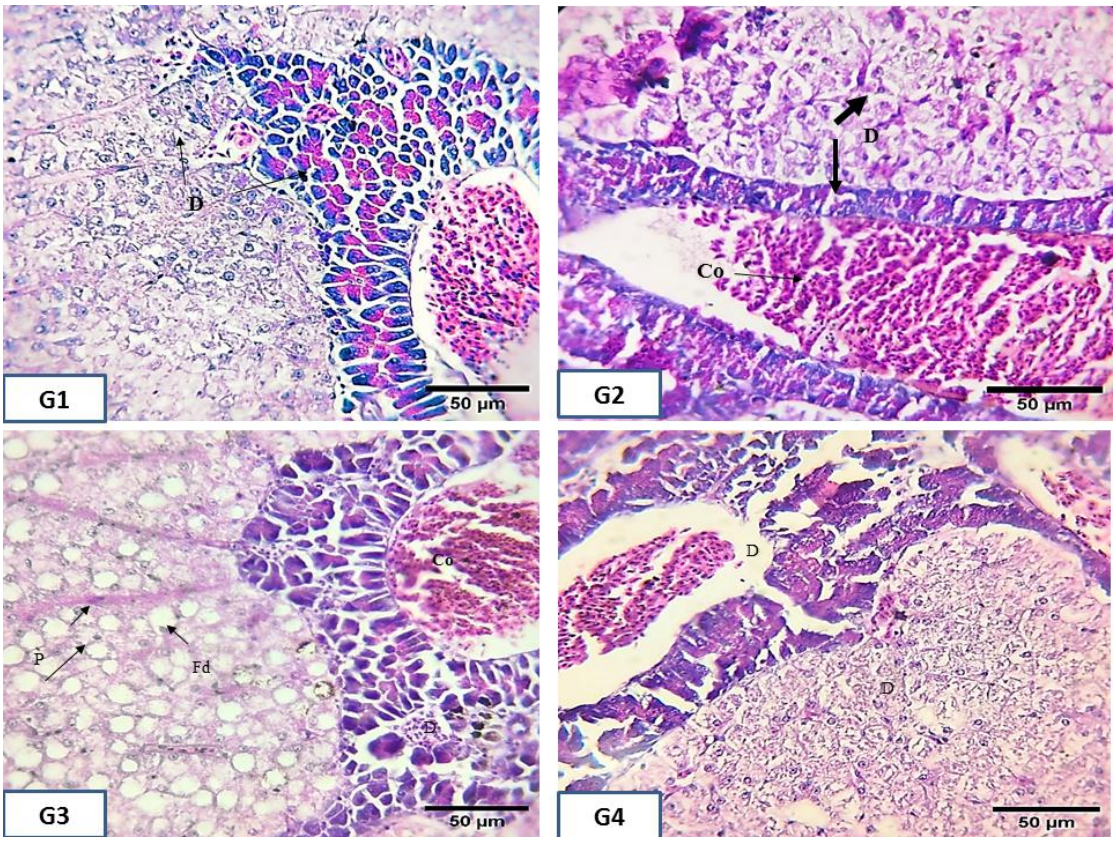


Figure 12. Histopathological sections of the liver and pancreas stained with hematoxylin and eosin (H&E) revealed various histopathological alterations among the examined groups. The phage-treated group (G2) showed degeneration of hepatic cells and pancreatic tissue (D), along with congestion and dilation of the hepatic vein (Co). The infected group (G3) exhibited marked congestion and dilation of the hepatic vein (Co) and hepatic sinusoids (arrow), degeneration of pancreatic tissue (D), and fatty degeneration of hepatocytes (Fd)

accompanied by pyknotic nuclei (P). The control group (G1) and the infected group treated with bacteriophage (G4) showed congested blood vessels (Co) and moderate degeneration of hepatic cells and pancreatic tissue (D).

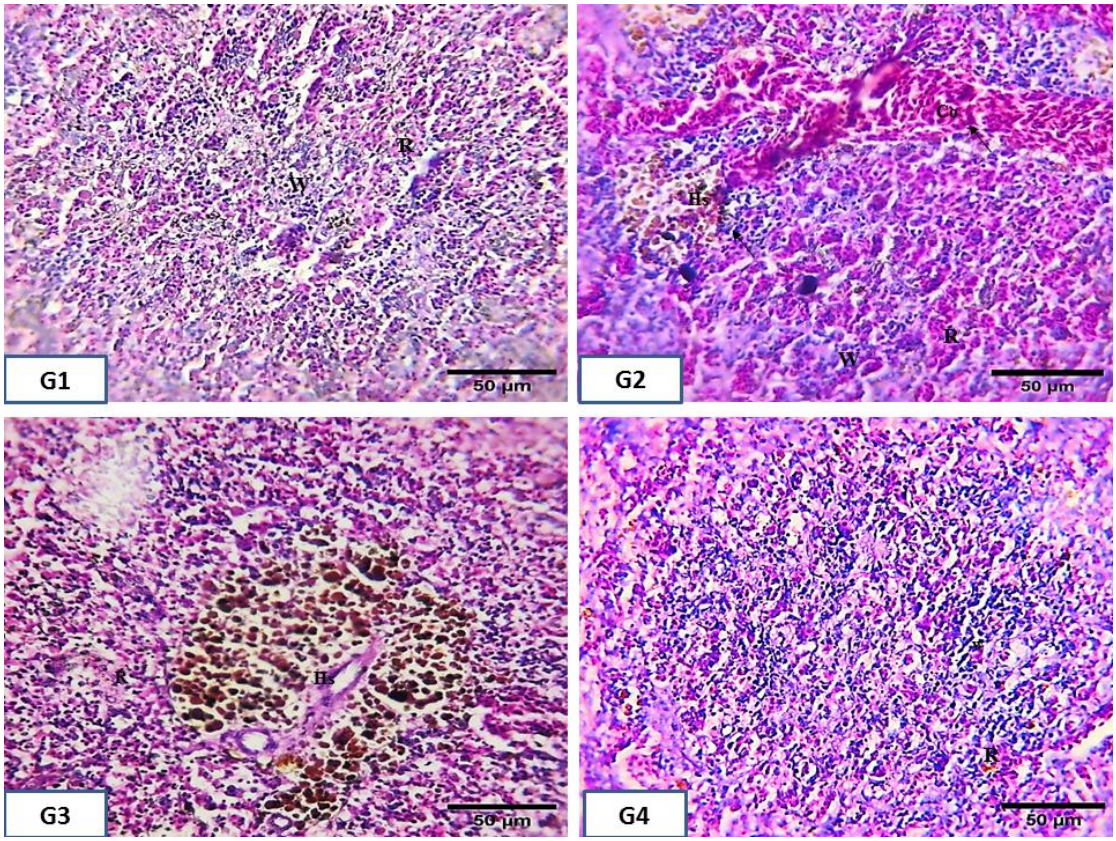


Figure 13. Histopathological sections of the spleen stained with hematoxylin and eosin (H&E) revealed distinct histological changes among the experimental groups. The phage-treated group (G2) showed blood congestion (Co), increased numbers of melanomacrophages (Hs), and an expansion of the red pulp (R). The infected group (G3) exhibited depletion of the white pulp (W), accompanied by an increase in the red pulp (R) and melanomacrophages (Hs). In contrast, the control group (G1) and the infected group treated with bacteriophage (G4) showed prominent white pulp (W), indicating a relatively preserved splenic architecture.

Supplementary Files

This is a list of supplementary files associated with this preprint. Click to download.

- Table.docx